J|A|C|S

A R T I C L E S

Stable Mechanistically-Relevant Aromatic-Based Carbenium Ions in Zeolite Catalysts

Louis A. Clark,[†] Marek Sierka,[‡] and Joachim Sauer*

*Contribution from the Institut für Chemie, Humboldt-Universität zu Berlin,
Unter den Linden 6, D-10099 Berlin, Germany*

Received August 29, 2002 ; E-mail: js@chemie.hu-berlin.de

Abstract: The existence of carbenium ion species is assumed in many zeolite catalysis mechanisms. Using computational techniques that include environmental effects, a benzenium-type carbenium ion is identified in zeolite catalysts for the first time. Localization of nearby transition states indicate that this species may play an important role as an intermediate in the bimolecular *m*-xylene disproportionation reaction. The barrier to back-donation of the proton from the benzenium ion is at least 50 kJ/mol, meaning that this species may be spectroscopically observable. An additional carbenium ion intermediate, formed by abstraction of a hydride from *m*-xylene, is also predicted. The stability of this second new carbenium ion suggests that aromatic-based carbenium ions are likely to be intermediates in many zeolite-catalyzed reactions. Two types of fundamentally different fully periodic calculations support the stability predictions.

Introduction

The role of carbenium ions in hydrocarbon conversion reactions over acidic zeolite catalysts is much debated. These cationic species form when a proton is added to an unsaturated hydrocarbon or as a result of hydride abstraction from a saturated carbon. It was first assumed that they were as common in zeolites as they are in homogeneous reactions.[1] However, NMR studies failed to find small carbenium ions such as allyl, isopropyl and *tert*-butyl as intermediates in zeolites.[2-4] Quantum chemistry calculations employing small cluster models[5,6] also came to the conclusion that these ionic species were only transition states, and it was accepted that only the surface-bound alkoxides were stable. Subsequently, several types of larger persistent carbenium ions were found, including cyclic, resonance-stabilized tertiary cations,[4,7,8] α,ω-diphenyl-substituted allylic and pentadienylium cations[9] and methyl-substituted benzenium ions.[10]

The work presented here identifies new stable catalytically relevant carbenium ions in zeolite catalysts for the first time

using computational techniques. In contrast to previous work on small cluster models, inclusion of the full zeolite environment is seen to stabilize carbenium ions. Previously, attempts to include the zeolite environment were made for *tert*-butyl as the largest species and either did not lead to a stable carbenium[11] or led to conflicting conclusions for different methods used.[12]

The carbenium ions examined are possible intermediates of the classical diphenylmethane-mediated mechanism of *m*-xylene bimolecular disproportionation.[1,13-15] During the initiation step, an adsorbed *m*-xylene reacts with the acidic proton to lose a methyl hydrogen and form an alkoxide **1** or a carbenium ion **2**.

$$ZOH + m - xylene(ads) \rightarrow$$
$$ZO - CH_2 - C_6H_4 - CH_3 \ \mathbf{1} + H_2 \ (1)$$

$$ZOH + m - xylene(ads) \rightarrow$$
$$ZO^- + CH_3 - C_6H_4 - CH_2 + (ads) \ \mathbf{2} + H_2 \ (2)$$

Once **1** or **2** has been formed, it catalyzes methyl-transfer reactions where the first step is reaction with a second adsorbed *m*-xylene to form an intermediate benzenium ion based on 3-methylphenyl-2,4-dimethylphenyl-methane **3**. To complete the

$$ZO - CH_2 - C_6H_4 - CH_3 \ + \ m - xylene(ads) \ \rightarrow$$
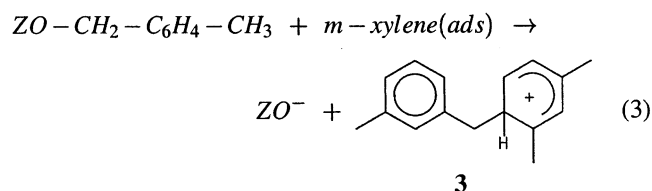
methyl transfer and produce a trimethylbenzene species, **3** must transfer its extra proton to the other ring and split off a trimethylbenzene (TMB) carbenium ion. This cation may then abstract a hydride from another *m*-xylene and desorb, leaving
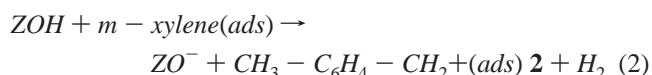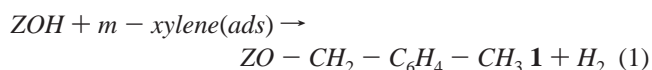
[†] E-mail: lc@chemie.hu-berlin.de.

[‡] Present address: Institut für Physikalische Chemie, Lehrstuhl für Theoretische Chemie, Universität Karlsruhe (TH), Kaiserstr. 12, D-76128 Karlsruhe, Germany.

(1) Olah, G. A.; Molnar, A. *Hydrocarbon Chemistry*; Wiley: New York, 1995.
(2) Aronson, M. T.; Gorte, R. J.; Farneth, W. E.; White, D. *J. Am. Chem. Soc.* **1989**, *111*, 840−846.
(3) Haw, J. F.; Richardson, B. R.; Oshiro, I. S.; Lazo, N. D.; Speed, J. A. *J. Am. Chem. Soc.* **1989**, *111*, 2052−2058.
(4) Haw, J. F.; Nicholas, J. B.; Xu, T.; Beck, L. W.; Ferguson, D. B. *Acc. Chem. Res.* **1996**, *29*, 259−267.
(5) Kazansky, V. B.; Frash, M. V.; van Santen, R. A. *Appl. Catal., A* **1996**, *146*, 225−247.
(6) Rigby, A. M.; Kramer, G. J.; van Santen, R. A. *J. Catal.* **1997**, *170*, 1−10.
(7) Yang, S. W.; Kondo, J. N.; Domen, K. *Chem. Commun.* **2001**, 2008−2009.
(8) Roduner, E.; Dilger, H. *J. Am. Chem. Soc.* **2001**, *123*, 7717−7718.
(9) Adam, W.; Casades, I.; Fornes, V.; Garcia, H.; Weichold, O. *J. Org. Chem.* **2000**, *65*, 3947−3951.
(10) Xu, T.; Barich, D. H.; Goguen, P. W.; Song, W. G.; Wang, Z. K.; Nicholas, J. B.; Haw, J. F. *J. Am. Chem. Soc.* **1998**, *120*, 4025−4026.
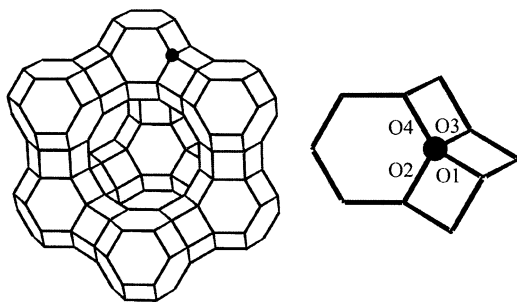
Figure 1. Depiction of the four crystallographically unique oxygen positions in the faujasite structure.

the alkoxide **1** or the carbenium ion **2** to continue the cycle. In this work, only the benzenium ion **3** that would split to form 1,2,4-TMB is considered.

Although cluster-based theoretical studies[16,17] of the related toluene disproportionation reaction give comparable energies for competing pathways, isotope-labeling experiments during toluene disproportionation provide evidence that the diphenyl-methane-mediated pathway is important even in the relatively confined environment of HZSM-5.[18] In this study the zeolite environment is the FAU-type framework with a single acidic site (Si/Al = 47). This relatively open framework can more easily accommodate the bulky biaromatic species, making the diphenylmethane-mediated pathway even more likely. While the position of the Al insertion into the FAU framework is unique, the AlO_4-tetrahedron has four crystallographically different O positions at which the acidic proton can sit (Figure 1). We assume here that the proton begins the reaction at the most stable O1 position (Figure 2) which gives rise to the so-called high-frequency OH band in the IR spectrum (see ref 19 and references therein). The alkoxide species then forms on the neighboring O4 position. In many of the remaining structures, the species are unbound, and therefore the oxygen positions are undifferentiated.

Large hydrocarbon species in zeolite catalysts with unit cells containing several hundred atoms are still a challenge for quantum chemistry methods. Density functional theory (DFT) renders such calculations possible, but they are still computationally very demanding and suffer from an additional problem. While current density functionals are well suited for bond breaking−bond making reaction steps, they fail to yield reliable energies for the van der Waals interactions which dominate the adsorption−desorption steps (see ref 20 and refs therein).

We make use of a simulation method capable of treating the full active-site environment at reasonable computational ex-

pense. The simulation technique is part of a family of mixed quantum mechanical−molecular mechanical (QM/MM) embedding techniques that are becoming more widely available.[21−23] It limits the quantum mechanical description to the zeolite active site and the reacting hydrocarbon molecules. The remainder of the interactions, including the zeolite environment and those between the hydrocarbon and zeolite, are handled using faster molecular mechanics force field calculations. Force field calculations are known to provide a good description of van der Waals interactions in general and of zeolite adsorption energies in particular.[24−26] Thus, the combined approach has two advantages compared to full DFT calculations. It reduces the computational effort significantly (enabling us to treat much larger systems), and it produces more reliable adsorption energies as we will show below.

The combined QM/MM method defines the potential energy surface as[27]

$$E(S)_{QM/MM} = E(S)_{MM} - E(C)_{MM} + E(C)_{QM} \qquad (4)$$

Here $E(S)_{QM/MM}$ is the composite QM/MM energy of the whole system, and $E(S)_{MM}$ is the MM energy of the whole system. The higher-accuracy description of the active site from the QM method is incorporated by subtracting out the MM results ($E(C)_{MM}$) in a small region on and around the active site, and replacing them by QM results in the same region ($E(C)_{QM}$). From this definition of the potential energy surface, consistent expressions are derived for combined gradients and second derivatives.

Figure 3 shows the partitioning of the system into the QM cluster and its environment. The zeolite cluster is a three T-atom model terminated with hydroxyl groups and having the chemical formula: $(OH)_2Al(OSi(OH)_3)_2$. This cluster is small enough to guarantee that the van der Waals interactions between the hydrocarbon and the zeolite are described by the force field (which is superior to DFT for this purpose). It is also large enough to describe bond-breaking and bond-making properly within the hybrid DFT/shell model potential scheme. This is known from previous calculations of deprotonation energies.[28−30] Cluster models consisting of three or even two T atoms, when embedded into a shell-model potential description of the zeolite framework, yield values that agree within a few kJ/mol with the limit obtained for very large embedded cluster models. Further support comes from comparison with full periodic DFT calculations in this study.

Computational Details

The noncubic FAU unit cell was used in this study. It contains 144 tetrahedral or oxygen atoms and, with one aluminum substitution, has a Si/Al ratio of 47. If a full cubic unit cell of 576 atoms has eight

(11) Sinclair, P. E.; Vries, A. D.; Sherwood, P.; Catlow, C. R. A.; Santen, R. A. V. *J. Chem. Soc., Faraday Trans.* **1998**, *94*, 3401−3408.
(12) Boronat, M.; Zicovich-Wilson, C. M.; Viruela, P.; Corma, A. *J. Phys. Chem. B* **2001**, *105*, 11169−11177.
(13) Olson, D. H.; Haag, W. O. In *Catalytic Materials Relationship Between Structure and Reactivity*; Whyte, T. E., Ed.; ACS Symposium Series 248; American Chemical Society: Washington, DC, 1984; pp 275−307.
(14) Tsai, T. C.; Liu, S. B.; Wang, I. *Appl. Catal., A* **1999**, *181*, 355−398.
(15) Guisnet, M.; Gnep, N. S.; Morin, S. *Microporous Mesoporous Mater.* **2000**, *35−36*, 47−59.
(16) Blaszkowski, S. R.; van Santen, R. A. In *Transition State Modeling for Catalysis*; Morokuma, K., Truhlar, D. G., Eds.; ACS Symposium Series 721; American Chemical Society: Washington, DC, 1999; pp 307−320.
(17) Rozanska, X.; Saintigny, X.; Santen, R. A. V.; Hutschka, F. *J. Catal.* **2001**, *202*, 141−155.
(18) Xiong, Y. S.; Rodewald, P. G.; Chang, C. D. *J. Am. Chem. Soc.* **1995**, *117*, 9427−9431.
(19) Sierka, M.; Sauer, J. *J. Phys. Chem. B* **2001**, *105*, 1603−1613.
(20) Wesolowski, T. A.; Parisel, O.; Ellinger, Y.; Weber, J. *J. Phys. Chem. A* **1997**, *101*, 7818−7825.

(21) *Combined Quantum Mechanical and Molecular Mechanical Methods*; Gao, J., Thompson, M. A., Eds.; ACS Symposium Series 712; American Chemical Society: Washington, DC, 1998.
(22) Mordasini, T. Z.; Thiel, W. *Chimia* **1998**, *52*, 288−291.
(23) Sauer, J.; Sierka, M. *J. Comput. Chem.* **2000**, *21*, 1470−1493.
(24) Snurr, R. Q.; Bell, A. T.; Theodorou, D. N. *J. Phys. Chem.* **1993**, *97*, 13742−13752.
(25) Gupta, A.; Clark, L. A.; Snurr, R. Q. *Langmuir* **2000**, *16*, 3910−3919.
(26) Fuchs, A. H.; Cheetham, A. K. *J. Phys. Chem. B* **2001**, *105*, 7375−7383.
(27) Sierka, M.; Sauer, J. *J. Chem. Phys.* **2000**, *112*, 6983−6996.
(28) Brändle, M.; Sauer, J. *J. Chem. Phys.* **1998**, *109*, 10379−10389.
(29) Sierka, M.; Eichler, U.; Datka, J.; Sauer, J. *J. Phys. Chem. B* **1998**, *102*, 6397−6404.
(30) For the O(1)H faujasite site, the B3LYP value of the deprotonation energy[29] was found to change by no more than 2 kJ/mol when extending the embedded cluster from 4 to 14 T.
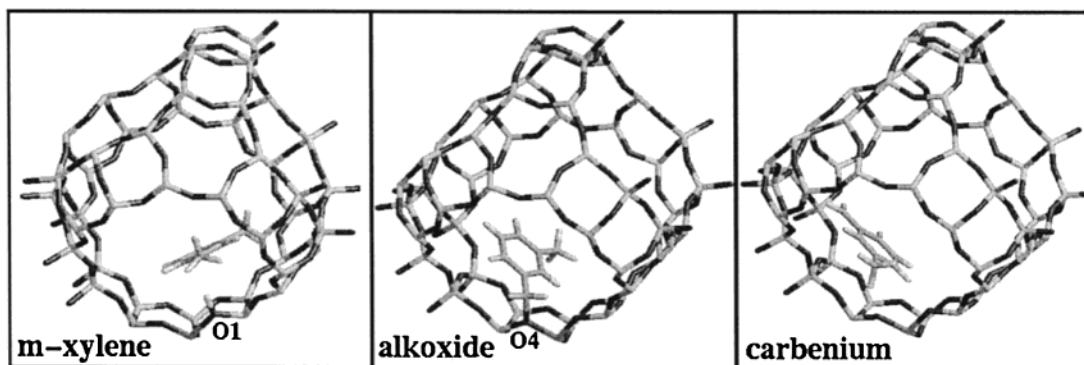
Figure 2. Illustration of the various *m*-xylene species structures. *m*-Xylene adsorbs at the acidic proton on the O1 site. A methyl hydrogen then reacts with the acidic proton to lose diatomic hydrogen and an alkoxide species is formed at the O4 position. This alkoxide may then convert to a free carbenium ion species.
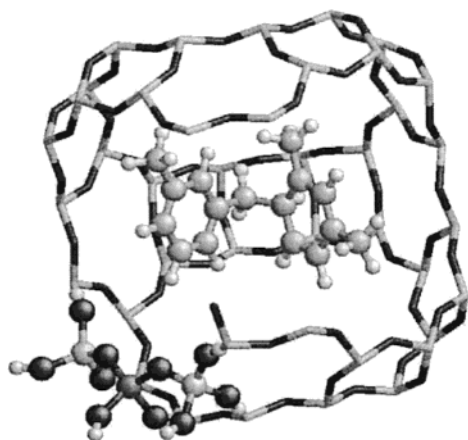

Figure 3. Partitioning of the system shown for the stable benzenium ion **3b** configuration. The QM portion of the calculation, including the hydrogen link-atoms, is displayed as balls and sticks. Most of the periodic MM-only portion is also shown and is displayed only as sticks.

supercages, our representation then has two. The cell has edge lengths of: $a = 17.4298$ Å, $b = 17.4925$ Å, $c = 17.4856$ Å and angles of: $\alpha = 59.8709°$, $\beta = 59.8981°$, $\gamma = 59.9960°$.

For the embedding method, DFT calculations were performed using the TURBOMOLE[31,32] program with the B3LYP functional[33−35] and DZP basis sets on all but the oxygen atoms, for which a TZP basis set was used.[36] MM calculations were done using a DFT-parametrized shell model for the zeolite[37] and the program GULP.[38] The use of the core−shell representation of the oxygen atoms makes the model polarizable and able to reproduce experimental infrared spectra.

Zeolite-adsorbate force field parameters were a combination of Lennard-Jones terms from the literature[39] and Coulombic charges from fits to the QM electrostatic potential. Lennard-Jones interactions act only between the hydrocarbon atoms and the zeolite oxygens. The parameters were taken from previous work and have been shown to reproduce adsorption well with similar charges.[24] A low-loading adsorption simulation of benzene with a shell model optimized silicalite framework and charges reproduced published results well, giving us confidence that the high charges on the lattice atoms do not compromise the force field. We do not perform force field evaluations for

intramolecular interactions because they subtract out in the final determinations of the QM/MM interactions.

The fixed point-charges on each hydrocarbon species are best fit to reproduce electrostatic interactions with point-charges in a boundary region around the molecules using Gaussian98.[40] These charges are rounded to the nearest 0.1 increment and constrained to reproduce the total charge on the molecules. For single-ring neutral species, such as *m*-xylene we use the most common charges for the carbon atoms.[41] Methyl group carbons, unsubstituted ring carbons, and substituted ring carbons have charges of −0.3, −0.1, and 0.0, respectively. We find that these commonly used charges are similar to those obtained from an electrostatic fit. All atomic charges are provided in the Supporting Information.

To blend the interactions produced by the point-charge differences between a given reactant and product we employ a simple 2×2 version of the empirical valence bond (EVB)[42] method described in more detail elsewhere.[27] This EVB methodology is used for location of the transition states. The energy and derivatives are calculated using eqs 5 and 10 in ref 27. In this work we use only a single internal coordinate to define the transition-state position, and the equation for the coupling element (V_{12}) reduces to:

$$(V_{12})^2 = A \exp\left(\frac{1}{2} C(\Delta q)^2\right) \tag{5}$$

Here $\Delta q = q - q_0$ where q is the internal coordinate representing the reaction pathway and q_0 is the value at the transition state. Because this EVB blending of the two charge distributions only affects the environment, the calculations are quite insensitive to the adjustable A and C parameters. We find that, for an A value of 10.0 eV, the energy does not change significantly even if adjustments spanning an order of magnitude are made. Similarly, the results are insensitive to changes in the C value of −10.0 Å^{-1} a factor of 2 lower or at least 2 orders of magnitude higher. The q_0 parameter can significantly affect the final energies if it is outside a 0.2−0.3 Å range from the transition state. For this reason, it may be necessary to change the q_0 during a transition-state optimization. To reproduce the end-point energies with the EVB

(31) Ahlrichs, R.; Bär, M.; Häser, M.; Horn, H.; Kölmel, C. M. *Chem. Phys. Lett.* **1989**, *162*, 165.
(32) Treutler, O.; Ahlrichs, R. *J. Chem. Phys.* **1995**, *102*, 346−354.
(33) Becke, A. D. *Phys. Rev. A* **1988**, *38*, 3908−3100.
(34) Lee, C.; Yang, W.; Parr, R. G. *Phys. Rev. B* **1988**, *37*, 785−789.
(35) Becke, A. D. *J. Chem. Phys.* **1993**, *98*, 5648−5652.
(36) Schäfer, A.; Horn, H.; Ahlrichs, R. *J. Chem. Phys.* **1992**, *97*, 2571−2577.
(37) Sierka, M.; Sauer, J. *Faraday Discuss.* **1997**, *106*, 41−62.
(38) Gale, J. D. *J. Chem. Soc., Faraday Trans.* **1997**, *93*, 629−637.
(39) These parameters are: $\sigma_{H-O} = 2.6059$ Å, $\epsilon_{H-O} = 49.0901$ K, $\sigma_{C-O} = 3.0068$, $\epsilon_{C-O} = 73.5985$.

(40) Frisch, M. J.; Trucks, G. W.; Schlegel, H. B.; Scuseria, G. E.; Robb, M. A.; Cheeseman, J. R.; Zakrzewski, V. G.; Montgomery, J. A., Jr.; Stratmann, R. E.; Burant, J. C.; Dapprich, S.; Millam, J. M.; Daniels, A. D.; Kudin, K. N.; Strain, M. C.; Farkas, O.; Tomasi, J.; Barone, V.; Cossi, M.; Cammi, R.; Mennucci, B.; Pomelli, C.; Adamo, C.; Clifford, S.; Ochterski, J.; Petersson, G. A.; Ayala, P. Y.; Cui, Q.; Morokuma, K.; Malick, D. K.; Rabuck, A. D.; Raghavachari, K.; Foresman, J. B.; Cioslowski, J.; Ortiz, J. V.; Baboul, A. G.; Stefanov, B. B.; Liu, G.; Liashenko, A.; Piskorz, P.; Komaromi, I.; Gomperts, R.; Martin, R. L.; Fox, D. J.; Keith, T.; Al-Laham, M. A.; Peng, C. Y.; Nanayakkara, A.; Gonzalez, C.; Challacombe, M.; Gill, P. M. W.; Johnson, B.; Chen, W.; Wong, M. W.; Andres, J. L.; Gonzalez, C.; Head-Gordon, M.; Replogle, E. S.; Pople, J. A. *Gaussian98*, revision a.7; Gaussian, Inc.: Pittsburgh, PA, 1988.
(41) Hagler, A. T.; Lifson, S.; Dauber, P. *J. Am. Chem. Soc.* **1979**, *101*, 5122. (as implemented in the Discover software of Accelrys Inc.).
(42) Aqvist, J.; Warshel, A. *Chem. Rev.* **1993**, *93*, 2523−2544.

Table 1: Comparison of Relevant Reaction Energies Generated from QM/MM Embedding[a] and Full QM Planewave Calculations

| | energies in kJ/mol | | | |
quantity	QM/MM	QM	MM	full QM
	Reaction Energies			
m-xylene(gas) → *m*-xylene(ads) O(1)-position	−52	−17	−35	-
m-xylene(gas) → *m*-xylene(ads) O(4)-position	−61	−12	−49	−28
alkoxide **1** O(4) → carbenium **2**	53	164	−111	63
	Deprotonation Energies			
zeolite (O(1)H → O⁻)	1155	1321	−166	-
zeolite (O(4)H → O⁻)	1133	1320	−187	1174
carbenium **2**[b]	n.a.	1028[b]	n.a.	1007
benzenium **3**[c]	n.a.	862	n.a.	859

[a] The embedding energies are also broken into QM and MM contributions. [b] Yielding $CH_2 = C_6H_4 = CH_2$ with a triplet ground state (biradical). [c] Yielding 3-methylphenyl-2,4-dimethylphenyl-methane.

we find it necessary to include at least one spring-constant in each end-point state on a bond that changes during the reaction.

All structures were optimized to minima or first-order saddle points using the QMPOT driver code.[27] Analytical second derivative calculations were performed on the final structures to verify the type of stationary point. Gradients were converged to less than 5.0×10^{-3} eV/Å for the maximum component. Due to the size of the system and the flat potential surface, it was not unusual for the optimizations to require 400 or more quasi-Newton steps for convergence.

Computationally more demanding full DFT planewave calculations were done for comparison using the CPMD code[43] with the PBE functional,[44] Troullier−Martins pseudopotentials and a plane wave basis set up to a cutoff of 70 Rydberg. This methodology is different from that of QM cluster calculations and cannot be expected to give exactly the same result. The PBE functional, a modification of the PW91 functional, is adopted since the exact exchange part in the B3LYP hybrid functional cannot be efficiently calculated with planewave basis sets. Gradient corrected functionals such as PBE are generally less accurate than hybrid functionals such as B3LYP. The rms errors in the energies of atomization are about 35 kJ/mol for PBE[45,46] and about 10−20 kJ/mol for B3LYP.[46]

Results and Discussion

To ascertain the reliability of our methodology, we compare reaction energies generated using the QM/MM embedding method with those from the computationally more demanding full DFT planewave calculations. Within limitations due to the different functionals and basis sets, we expect the two methods to yield similar results for reactions inside zeolite channels where changes in the van der Waals interactions are minor. For other reactions, particularly those involving adsorption or desorption, the QM/MM embedding technique is expected to be an improvement because van der Waals interactions are included as a part of the force field. Table 1 shows results that support these predictions.

An estimate for the electronic energy of adsorption derived from available experimental heats of adsorption[47−50] and from

(43) Hutter, J.; Alavi, A.; Deutsch, T.; Bernasconi, M.; Goedecker, S.; Marx, D.; Tuckerman, M.; Parrinello, M. *CPMD 3.4.1*; MPI für Festkörperforschung and IBM Zurich Research Laboratory, 1995−1999.
(44) Perdew, J. P.; Burke, K.; Ernzerhof, M. *Phys. Rev. Lett.* **1996**, *77*, 3865−3868.
(45) Matveev, A.; Staufer, M.; Mayer, M.; Rösch, N. *Int. J. Quantum Chem.* **1999**, *75*, 4−5.
(46) Cramer, C. J. *Essential of Computational Chemistry: Theories and Models*; Wiley: Chicester, 2002; p 261−263.
(47) Schirmer, W.; Thamm, H.; Stach, H.; Lohse, U. In *The Properties and Applications of Zeolites*; Townsend, P. P., Ed.; The Chemical Society: London, 1980; Spec. Pub. No. 33, pp 204-213.
(48) Thamm, H. *J. Phys. Chem.* **1987**, *91*, 8−11.
(49) Choudhary, V. R.; Srinivasan, K. R.; Singh, A. P. *Zeolites* **1990**, *10*, 16−20.
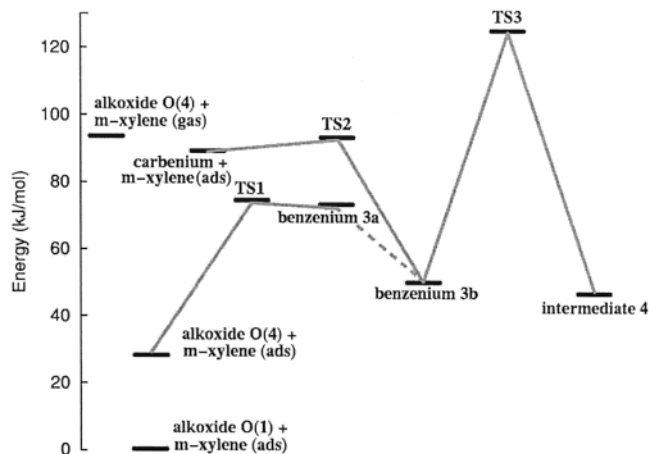(50) Jentys, A.; Lercher, J. personal communication. 2002.

Figure 4. Relative energies of the intermediates and transition-state structures near the diphenyl benzenium ion **3b**. The dotted line connecting the benzenium ion states **3a** and **3b** is an assumed low-barrier path, no transition-state structure has been located. Intermediate **4** is the 3-methyl-phenyl-2,4-dimethylphenyl-methane species.

calculated zero-point vibrational energies is −67 to −73 kJ/mol.[51] Full periodic DFT calculations have been made with the proton at the O(4) position. An unreasonable value of −28 kJ/mol is obtained, while the QM/MM calculations yield a more acceptable value of −61 kJ/mol. At the more stable O(1) position, the QM/MM adsorption energy is −52 kJ/mol, of which the largest share (−35 kJ/mol) comes from the force field (MM) part (see Table 1). This failure of periodic DFT for aromatics in zeolites has been observed before.[52,53]

The two different methods give comparable reaction energies for the alkoxide to carbenium ion transformation, with values of 53 and 63 kJ/mol coming from the embedding and full QM calculations, respectively. The similar energies for this reaction are expected since it occurs inside the zeolite pore and should involve little change in the van der Waals energy. This reaffirms the reliability of the QM/MM calculations.

(51) $\Delta E_{ads} = - q_{ads} + RT - \Delta E_{ZPE}$ The nearest available heats of adsorption are for benzene in H-FAU (45 kJ/mol)[47] and for benzene and xylenes in H-ZSM-5.[48−49] The latter suggest an increment of 20−22 kJ/mol for the additional CH_3 groups in xylene as compared to toluene. This results in an estimate of 65−67 kJ/mol for *m*-xylene in good agreement with 65−70 kJ/mol recently measured for *m*-xylene in H-FAU.[50] Using these most recent measurements, a zero-point energy contribution (ΔE_{ZPE}) of 5 kJ/mol and room temperature, we calculate an electronic energy of adsorption between −67 and −73 kJ/mol.
(52) Vos, A. M.; Rozanska, X.; Schoonheydt, R. A.; Santen, R. A. V.; Hutschka, F.; Hafner, J. *J. Am. Chem. Soc.* **2001**, *123*, 2799−2809.
(53) Demuth, T.; Benco, L.; Hafner, J.; Toulhoat, H.; Hutschka, F. *J. Chem. Phys.* **2001**, *114*, 3703−3712.
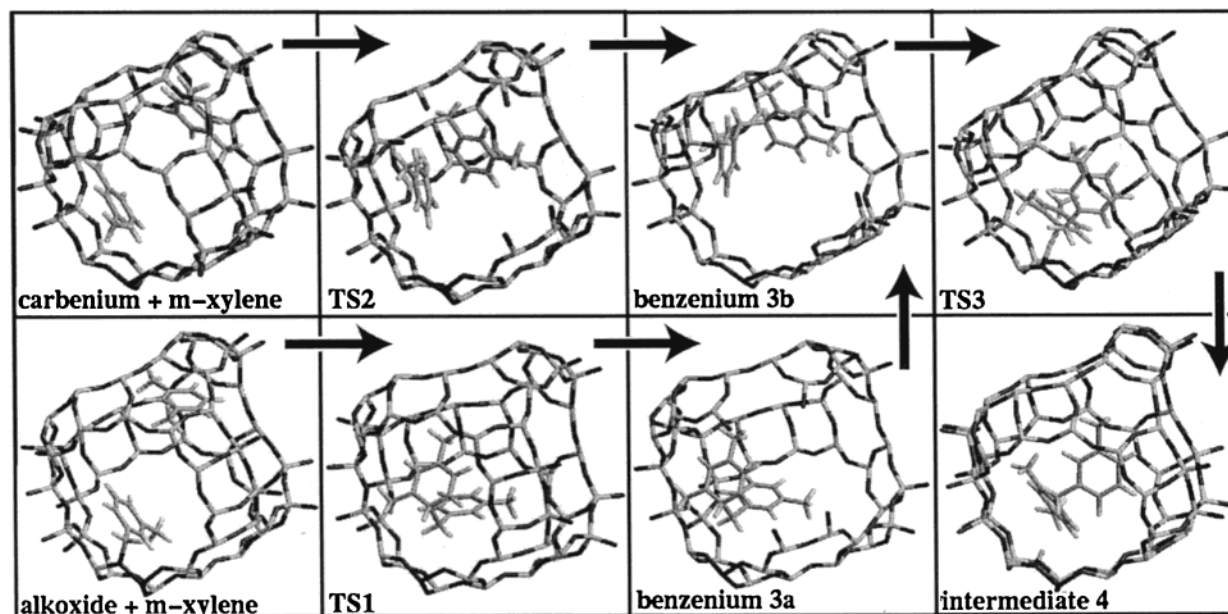
Figure 5. The reactants, intermediates, and transition states involved in the production of the 3-methylphenyl-2,4-dimethylphenyl-methane product.

The deprotonation energy obtained with the periodic QM calculation for faujasite is larger than the QM/MM result. This is an effect of the functional also found for other zeolites, e.g. for chabasite (CHA): 1192 kJ/mol (PBE),[54] and 1181 kJ/mol (B3LYP),[55] ZSM-5 (MFI, Al at T7, H at O17):[56] 1215 kJ/mol (PW91) 1200 kJ/mol (B3LYP). The errors in QM/MM results due to the small cluster size chosen are below 5 kJ/mol. In agreement with previous results[28,29] the deprotonation energies for O1 and O4 change from 1155 to 1151 kJ/mol and from 1133 to 1137 when the larger QM cluster models of ref 19 including eight T-atoms are used.

The most important result of our study is that *both the carbenium ion 2 and the benzenium ions 3a, 3b are stationary points* on both the combined QM/MM and the full QM potential energy surfaces. Reaction of the alkoxide and *m*-xylene channels the system into carbocation intermediates. The stability of the carbocations allows important reaction steps to occur at a much wider range of positions in the cavity than previously visualized. Figure 4 shows the relative energies of the intermediates and transition-state structures near the benzenium ion in the mechanism and Figure 5 shows the corresponding structures. A metastable intermediate **3a** near the acid site, very similar to the transition-state structure (TS1), is obtained from geometry optimization after perturbation of TS1 toward the products. The same species stabilized on the opposite side of the supercage, **3b**, may dissociate to form a carbenium ion and a *m*-xylene molecule via TS2 or may move back to the acidic site and lose its extra proton via TS3 to become 3-methylphenyl-2,4-dimethylphenyl-methane. Due to the stability of the carbocations and the their many degrees of freedom, there is likely to be many more similar minima and transition states.

Energies for the states depicted in Figures 4 and 5 are given in Table 2. It can be seen that there are only very small energetic

Table 2: Relative Potential Energies for the Intermediates and Transition-State Structures Shown in Figure 4 Broken into QM and MM Contributions[a]

state	system energies in kJ/mol		
	QM/MM	QM	MM
alkoxide O(4) + *m*-xylene(gas)	94	11	83
alkoxide O(4) + *m*-xylene(ads.)	30	11	19
alkoxide O(1) + *m*-xylene(ads.)	0	0	0
TS1	75	135	−60
benzenium 3a	74	135	−61
carbenium + *m*-xylene	90	181	−91
TS2	94	300	−206
benzenium 3b	50	272	−222
TS3	125	72	53
3-methylphenyl-2,4-dimethylphenyl-methane	47	−47	94

[a] The alkoxide O(1) + *m*-xylene (ads) state is taken to be the reference.

differences within the state-pairs [carbenium **2** + *m*-xylene]-[TS2] and [benzenium **3a**]-[TS1], indicating that the associated barriers of 4 and 1 kJ/mol will be very sensitive to the theoretical method used. From a practical viewpoint, this also means that conversion between the carbenium **2** + *m*-xylene state and the benzenium intermediates **3a** and **3b** is relatively facile and may result in isomerization.

Table 2 and Figure 4 show that there are significant barriers to the decomposition of the benzenium ion **3b** via TS2 (44 kJ/mol) or to the deprotonation via TS3 (75 kJ/mol). Since the smallest barrier to destruction of this cation is at least 44 kJ/mol, we suggest that it is kinetically stable. To verify this, the transition-state structure (TS3) was located with the full periodic DFT. The resulting barrier of 47 kJ/mol is qualitatively similar to that from the QM/MM calculations. It is also thermodynamically (meta-)stable since it is lower in energy than the alkoxide + *m*-xylene (gas) state.

Nicholas and Haw[57] have predicted that only species with proton affinities (PA) greater than approximately 874 kJ/mol persist in zeolites. The PA of 3-methylphenyl-2,4-dimethyl-

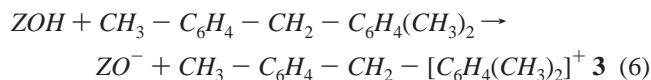(54) Tuma, C. Diplom Thesis, Humboldt-Universität, Berlin, 2000.
(55) Sauer, J.; Schröder, K. P.; Termath, V. *Collect. Czech. Chem. Commun.* **1998**, *63*, 1394−1408.
(56) Haase, F.; Sauer, J. *Microporous Mesoporous Mater.* **2000**, *35−6*, 379−385.
(57) Nicholas, J. B.; Haw, J. F. *J. Am. Chem. Soc.* **1998**, *120*, 11804−11805.

phenyl-methane is only 821 kJ/mol[58]—it remains to be seen if this is enough to observe the benzenium intermediate **3b** experimentally. Note also that the proposed PA cutoff is not a sufficient stability predictor if the carbenium ion can transform without losing a proton. One such case is the carbenium ion **2**. The PA of its generating olefin is 1031 kJ/mol,[58] indicating that it would not give back the proton to the zeolite, but it may transform to the more stable alkoxide **1**.

We can analyze the stabilizing effect of the zeolite environment by looking at the proton-transfer reaction that forms the benzenium cation, **3**.

$$ZOH + CH_3 - C_6H_4 - CH_2 - C_6H_4(CH_3)_2 \rightarrow$$
$$ZO^- + CH_3 - C_6H_4 - CH_2 - [C_6H_4(CH_3)_2]^+ \; \textbf{3} \quad (6)$$

In the absence of adsorbate−zeolite interactions, the difference of the proton affinities of the zeolite and the 3-methyl-phenyl-2,4-dimethylphenyl-methane gives the reaction energy. The higher proton affinity of the zeolite dictates that the reaction energy would be +293 kJ/mol. Table 2 shows that this energy is actually +3 kJ/mol for benzenium structure **3b** when zeolite−sorbate interactions are included. This stabilization by 290 kJ/mol compared to the gas-phase reaction has two contributions, one is the ionic attraction between the negatively charged deprotonated site and the positively charged benzenium ion and the other is the vdW (dispersion) interaction with the zeolite wall. The ionic interactions are predominantly included in the QM part (140 kJ/mol), while the MM portion (150 kJ/mol) contains most of the dispersion. A glance at Table 2 shows that the TS2 structure is also substantially stabilized by the MM contribution.

Dramatic shifts in the QM- and MM-stabilizing contributions are possible when adsorbates adopt different positions in the zeolite cavity. Benzenium ion structure **3a** is only 27 kJ/mol less stable than structure **3b**, but the total stabilization (266 kJ/mol with respect to gas-phase reaction) is dominated by ionic interactions, as the QM contribution of 277 kJ/mol indicates (the MM part is slightly destabilizing at 10 kJ/mol). In Figure 5, it can been seen that benzenium **3a** maximizes its QM interactions by siting near the negatively charged and deprotonated site. Conversely, benzenium **3b** fits tightly to the zeolite wall far from the active site where it maximizes the vdW interactions with the zeolite wall.

Conclusions

We have shown that aromatic-based carbenium ions are metastable intermediates on the potential energy surface and that both ionic and vdW (dispersion) interactions contribute to their stabilization in zeolite cavities. These species may also play a significant role in the diphenylmethane-mediated pathway of the *m*-xylene disproportionation reaction. Due to its stability, the diphenyl benzenium ion may repeatedly form, dissociate into the carbenium and *m*-xylene states, and then reform in a sterically different geometry before it further reacts. The stability also means that many of the important reaction steps may take place farther from the acid site than previously thought.

The calculations of the full zeolite environment were made possible by the development of a mixed QM/MM embedding method. This embedding method is compared to full QM planewave-based calculations and shown both to reproduce species stabilities and also to provide an improved description of adsorption energies.

Supporting Information Available: Complete set of atomic point charges (PDF). Structures and absolute energies for all stationary points (TXT). This material is available free of charge via the Internet at http://pubs.acs.org.

JA0283302

(58) Proton affinities have been estimated according to PA = ΔE(deprot) + ΔE(ZPVE)(B3LYP/DZP) + 5 kJ/mol. The increment of 5 kJ/mol accounts for all thermal effects at 298 K. ΔE(deprot) = ΔE(MP4-SDTQ/6-311+G*//B3LYP/DZP) = 844 kJ/mol for 3-methylphenyl-2,4-dimethylphenyl-methane. ΔE(deprot) = ΔE(CCSD(T)/6-311+G*//B3LYP/DZP) = 1042 kJ/mol for the precursor of carbenium **2** (triplet). These protocols reproduce the PA values of Nicholas and Haw[57] based on MP4-SDTQ within 5 kJ/mol. MP4 and CCSD(T) energies have been calculated with MOLPRO.[59]

(59) Hampel, C.; Peterson, K. A.; Werner, H. J. *Chem. Phys. Lett.* **1992**, *190*, 1−12 and refs therein. MOLPRO is a package of ab initio programs written by Werner, H.-J.; Knowles, P. J. with contributions from Almlof, J.; Amos, R. D.; Berning, A.; Deegan, M. J. O.; Eckert, F.; Elbert, S. T.; Hampel, C.; Lindh, R.; Meyer, W.; Nicklass, A.; Peterson, K.; Pitzer, R.; Stone, A. J.; Taylor, P. R.; Mura, M. E.; Pulay, P.; Schuetz, M.; Stoll, H.; Thorsteinsson, T.; Cooper, D. L.